Editors' Suggestion

Wide Critical Fluctuations of the Field-Induced Phase Transition in Graphite

Christophe Marcenat,[1] Thierry Klein,[2] David LeBoeuf,[3] Alexandre Jaoui,[4,5] Gabriel Seyfarth,[3] Jozef Kačmarčík,[6] Yoshimitsu Kohama,[7] Hervé Cercellier,[2] Hervé Aubin,[8] Kamran Behnia,[5] and Benoît Fauqué[4,*]

[1]*Université Grenoble Alpes, CEA, IRIG, PHELIQS, LATEQS, F-38000 Grenoble, France*
[2]*Université Grenoble Alpes, CNRS, Grenoble INP, Institut Néel, F-38000 Grenoble, France*
[3]*Laboratoire National des Champs Magnétiques Intenses (LNCMI-EMFL), CNRS, UGA, UPS, INSA, 38042 Grenoble/Toulouse, France*
[4]*JEIP, USR 3573 CNRS, Collège de France, PSL Research University, 11, Place Marcelin Berthelot, 75231 Paris Cedex 05, France*
[5]*Laboratoire de Physique et Etude des Matériaux (CNRS/UPMC), Ecole Supérieure de Physique et de Chimie Industrielles, 10 Rue Vauquelin, 75005 Paris, France*
[6]*Centre of Low Temperature Physics, Institute of Experimental Physics, Slovak Academy of Sciences, Watsonova 47, SK-04001 Košice, Slovakia*
[7]*The Institute of Solid State Physics, University of Tokyo, Kashiwa, Chiba 277-8581, Japan*
[8]*Centre de Nanosciences et de Nanotechnologies, CNRS, Université Paris-Saclay, 91120 Palaiseau, France*

(Received 11 November 2020; accepted 28 January 2021; published 8 March 2021)

In the immediate vicinity of the critical temperature (T_c) of a phase transition, there are fluctuations of the order parameter that reside beyond the mean-field approximation. Such critical fluctuations usually occur in a very narrow temperature window in contrast to Gaussian fluctuations. Here, we report on a study of specific heat in graphite subject to a high magnetic field when all carriers are confined in the lowest Landau levels. The observation of a BCS-like specific heat jump in both temperature and field sweeps establishes that the phase transition discovered decades ago in graphite is of the second order. The jump is preceded by a steady field-induced enhancement of the electronic specific heat. A modest (20%) reduction in the amplitude of the magnetic field (from 33 to 27 T) leads to a threefold decrease of T_c and a drastic widening of the specific heat anomaly, which acquires a tail spreading to two times T_c. We argue that the steady departure from the mean-field BCS behavior is the consequence of an exceptionally large Ginzburg number in this dilute metal, which grows steadily as the field lowers. Our fit of the critical fluctuations indicates that they belong to the $3DXY$ universality class as in the case of the ^{4}He superfluid transition.

DOI: 10.1103/PhysRevLett.126.106801

A phase transition is accompanied by sharp discontinuities of thermodynamic properties. Quantifying entropy by measuring the specific heat across the transition pins down the order of the transition and informs the underlying microscopic interaction. Of particular interest is the critical regime of the phase transition, which allows one to identify the universality class of the transition and provides information on the order parameter [1]. Critical fluctuations are important when their amplitude is comparable to the amplitude of the jump of the specific heat ΔC, which occurs roughly when the reduced temperature $\tau = T - T_c/T_c$ is smaller than τ_G [2], the Ginzburg criterion:

$$\tau_G = \alpha^2 \left(\frac{k_B}{\Delta C \xi_m^3} \right)^2. \quad (1)$$

Here, ξ_m is the average correlation length, and $\alpha = 1/4\sqrt{2}\pi$ is a numerical factor. In most cases, $\tau_G \ll 1$, the critical fluctuations are located in the extreme vicinity of the transition and therefore hardly observable. One notorious exception is the ^{4}He superfluid transition for which the shape of the transition is determined by critical fluctuations [3]. Near a quantum critical point, thermal fluctuations are replaced by quantum mechanical zero-point fluctuations, which can produce new quantum phases [4].

Here, we report on the electronic specific heat (C_{el}) of graphite, using state-of-the-art calorimeters, when all carriers are confined in the lowest Landau level (LLL), the so-called quantum limit, which can be easily achieved in this dilute metal. We find that this regime is marked by a steady field-induced enhancement of C_{el}, signaling the enhancement of electron-electron correlations. Deep in this regime, we detect a jump in C_{el}, unambiguously establishing a second-order phase transition induced by the magnetic field. As the magnetic field decreases, the anomaly shifts to a lower temperature and widens. It evolves from a BCS mean-field-type transition at 33 T to a crossover regime below 25 T. At the lowest critical temperature ($T_c \sim 1$ K), fluctuations can be observed up to two times T_c. We identify these fluctuations as critical fluctuations associated with an exceptionally large Ginzburg number. In contrast

with other phase transitions where a large critical regime of fluctuations is observed when correlation lengths are short, here the diluteness of the Fermi surface produces the extended regime of critical fluctuations. Our measurements are a first step toward thermodynamic studies of the numerous field-induced phases of dilute metals and their critical regimes (in cases where those regimes are observable).

With an electronic density as low as $n = 4 \times 10^{18}$ cm^{-3} and light in-plane mass carrier ($m^{\star}_{a,b} = 0.05$ m$_0$), a magnetic field of 7.5 T, labeled B_{QL}, oriented along the c axis is large enough to confine the carriers into the LLL ($n = 0$). In the early 1980s, the onset of an electronic phase transition at $B = 25$ T and $T = 1.3$ K was discovered [5]. Since then, extensive electrical [6–11], thermoelectrical [12], and ultrasound measurements [13] in a high magnetic field have established that graphite hosts a succession of at least two field-induced phases [7,11] arising from electron-hole instabilities. Depending on the nesting vector considered and the strength of the electron-electron interaction, various types of charge [10,14], spin density waves [15], or excitonic insulating phases [8,9,11,16] have been proposed. With the notable exception of ultrasound measurements [13], these studies have employed transport probes. Because of the low electronic density of graphite, thermodynamic studies are challenging but nevertheless crucial.

Figure 1(a) shows the field dependence of $\gamma = C_{\mathrm{el}}/T$ at $T = 1.6$ K up to 35 T of graphite. Electronic specific heat has been extracted from the total specific heat after substraction of the phononic contribution determined by the zero field measurement (see [17] for further details and the specific heat setup). At zero field, γ is as small as $20 \pm 3\ \mu\mathrm{J} \cdot \mathrm{mol}^{-1} \cdot \mathrm{K}^{-2}$ in good agreement with the value expected from the Slonczewski-Weiss-McClure band model [21,22]. This is several orders of magnitude smaller than in metals due to the low density and the lightness of carriers. Sweeping the magnetic field, we found that γ peaks at each Landau level depopulation. Above B_{QL}, γ increases linearly up to 28 T, where it presents yet another peak that evolves with temperature. The temperature and magnetic field dependence of the 28 T peak can be tracked by field sweeps (at different temperatures), as shown in the inset of Fig. 1, and by temperature sweeps (in different magnetic fields), as shown in Fig. 2(a).

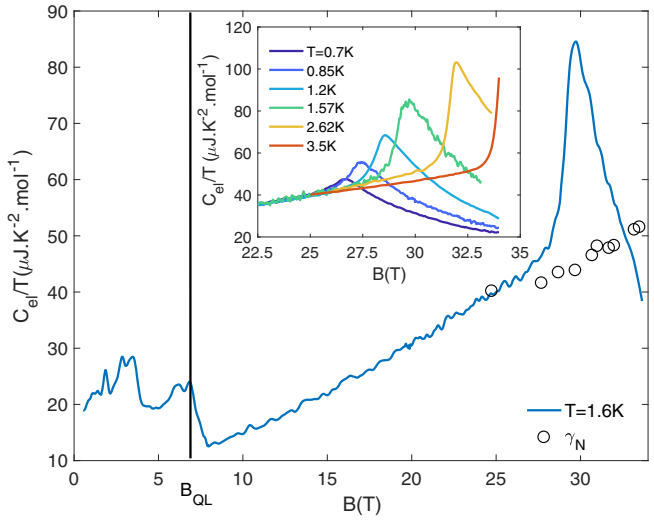

FIG. 1. Field dependence of $\gamma = C_{\mathrm{el}}/T$ at $T = 1.6$ K. The vertical black line indicates the quantum limit (QL) regime. When $B > B_{\mathrm{QL}} = 7.5$ T, holes and electrons are confined to their $n = 0$ Landau levels. Open circles represent γ in the normal state (labeled γ_N) deduced from temperature sweeps shown in Fig. 2. Inset: field sweeps at different temperatures.

We first comment on the evolution of γ with a magnetic field between 10 and 35 T. The magnitude of γ in the normal state, γ_N, deduced from temperature sweeps [Fig. 2(a)] and is represented by open black circles in Fig. 1. γ_N increases linearly with the magnetic field. The threefold enhancement between 10 and 35 T is larger than the enhancement of γ reported in $Sr_3Ru_2O_7$ across its quantum critical point [23]. This remarkable enhancement is driven by the change of the density of states (DOS) induced by the magnetic field. When $B > B_{\mathrm{QL}}$, the DOS of the LLL is the product of the in-plane

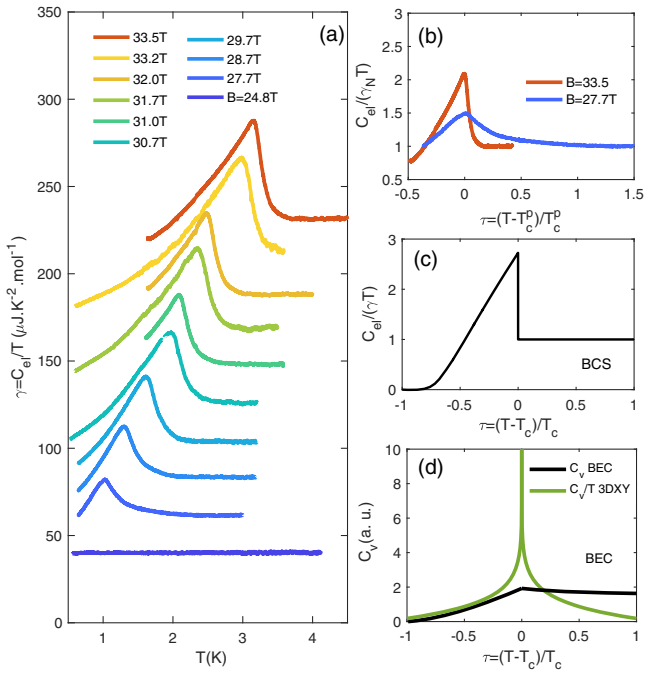

FIG. 2. Temperature dependence of γ. (a) $\gamma = C_{\mathrm{el}}/T$ as function of temperature for different magnetic fields. Curves are shifted for clarity. (b) $C_{\mathrm{el}}/\gamma_N T$ as function of $\tau = T - T_c^p/T_c^p$, where T_c^p is the temperature of the peak position. At $B = 27.7$ T, the tail of the transition extends up to twice T_c. (c) Specific heat anomaly for a BCS transition. The amplitude of the jump at T_c is such that $\Delta C_{\mathrm{el}}(T_c)/\gamma_N T_c = 1.43$ where $\Delta C_{\mathrm{el}}(T) = C_{\mathrm{el}}(T) - \gamma_N T$. (d) Specific heat anomaly in a Bose-Einstein condensation transition (in black) and the singularity caused by a $3DXY$ critical fluctuation (in green) like in the λ transition in helium.

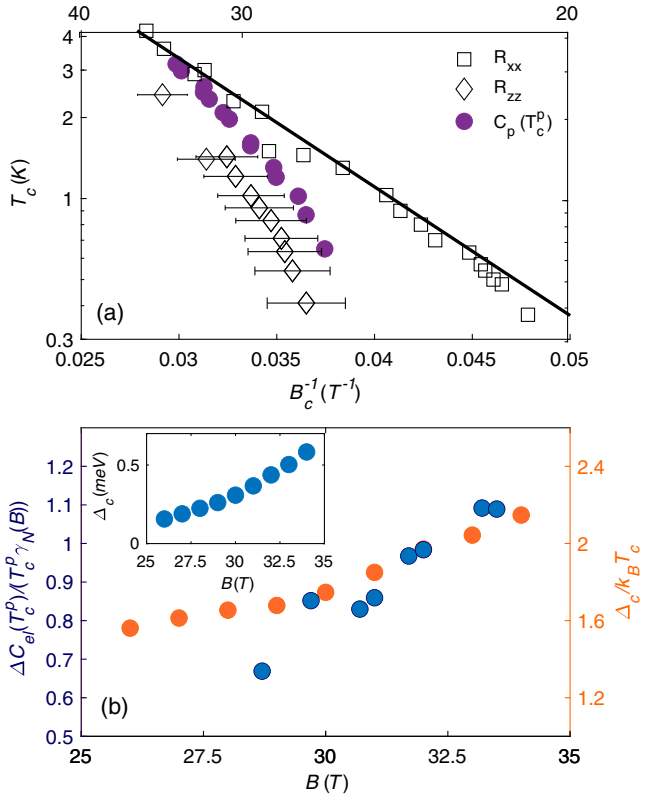

FIG. 3. (a) Phase diagram of graphite showing the evolution of critical temperature (T_c) as a function of the inverse of the magnetic field (B_c^{-1}) according to different experimental probes. Anomalies in R_{xx} (black open square points) and R_{zz} (black open diamond points) (from [13]) are compared to peaks in C_{el} (T_c^p in purple closed circles). The black line represents $T_c = T^\star \exp(-B^\star/B_c)$ and reasonably describes the evolution of R_{xx} anomalies. (b) Field dependence of $\Delta C_{el}(T_c^p)/\gamma_N T_c^p$ and $\Delta_c/k_B T_c$. Δ_c is the activation gap deduced from the c-axis resistance measurements (see [17]). Inset: Δ_c vs B.

degeneracy (which scales linearly with the field) and the one-dimensional DOS along the field direction. As long as the Fermi energy (E_F) is far from the bottom of the LLL, $\gamma_N \propto B$ with $\partial\gamma_N/\partial B \propto \sqrt{(m_z^\star/E_F)}$ where $m_z^\star$ is the mass along the magnetic field (see [17]). The small $E_F \simeq 40$ meV and the large c-axis mass $m_c^\star \simeq 10$–$20\ m_0$ of graphite set the large slope, which we find to be $\partial\gamma_N/\partial B = 2.2 \pm 0.5\ \mu J \cdot K^{-2} \cdot mol^{-1} \cdot T^{-1}$. Decades ago, starting from the Slonczewski-Weiss-McClure model, Jay-Gerin computed $\partial\gamma_N/\partial B = 1.8\ \mu J \cdot K^{-2} \cdot mol^{-1} \cdot T^{-1}$ [24] in quantitative agreement with our result.

At the highest magnetic field ($B = 33.5$ T), specific heat peaks at $T \simeq 3$ K [see Fig. 2(a)]. The transition shifts to a lower temperature with a decreasing magnetic field in contrast to a superconducting transition. By reducing the magnetic field by 20%, i.e., from 33.5 to 27.7 T, T_c^p (the temperature at which the specific heat peaks) decreases by a factor of 3. Figure 3(a) shows how T_c^p compares to T_c deduced from anomalies in the in-plane and out-of-plane resistance measurements, labeled R_{xx} and R_{zz}, respectively. Each symbol represents a $T_c(B)$ [or $B_c(T)$] anomaly. The vertical axis shows $\ln(T)$ and the horizontal axis B^{-1}. Thus, the BCS-like expression $T_c = T^\star \exp(-B^\star/B_c)$ [14] becomes a straight line, which reflects the behavior of $T_c(B)$ according to R_{xx} measurements. In this formula, $T^\star$ and $B^\star$ are phenomenological temperature and field scales, and the underlying assumption is that the DOS linearly increases with the magnetic field [14]. The onset of ordering has different manifestations in R_{xx}, which jumps by 30% but does not diverge, and in R_{zz}, which shows an activation behavior [7,11]. As seen in Fig. 3(a), the peak in C_{el}/T tracks the onset of the activation energy in R_{zz}, and below 3 K, they both occur below the R_{xx} anomaly and the BCS line. Figure 3(b) shows the evolution of the ratio of the activation gap Δ_c to the critical temperature with the magnetic field, which is close to what is expected in the BCS picture. Δ_c is deduced from a fit of R_{zz} of the form $R_{zz} \propto \exp(\Delta_c/k_B T)$ (see [17] for further details). $\Delta_c/k_B T_c$ weakens with decreasing field. Figure 3(a) shows that the normalized specific heat jump at T_c^p, $\Delta C_{el}(T_c^p)/\gamma_N T_c^p$ with $\Delta C_{el}(T) = C_{el}(T) - \gamma_N T$, presents a similar evolution toward weak coupling as the field decreases.

The steady evolution toward weak coupling with a decreasing magnetic field is accompanied by a drastic change in the shape of the specific heat anomaly [see Figs. 2(a) and 2(b)]. At $B = 33.5$ T, the amplitude of the jump is $\Delta C_{el}(T_c^p)/\gamma T_c^p = 1.1$ [see Fig. 3(b)], which is smaller than what is expected for a mean-field weak-coupling case and has a small tail caused by fluctuations above T_c^p. With decreasing T_c, the transition widens, $\Delta C_{el}(T_c^p)/\gamma T_c^p$ decreases, and the tail extends to higher temperatures. At $B_c = 27.7$ T, the tail of the transition extends up to twice T_c^p. The anomalies at two fields differing by a mere factor of 1.2 are compared in Fig. 2. At $B = 33.5$ T, the anomaly looks similar to a mean-field BCS transition [Fig. 2(c)], but at $B_c = 27.7$ T it acquires a cusp shape, and the fluctuating contribution weighs as much as the mean-field jump. This is to be compared to and contrasted with the case of the superfluid transition in ^{4}He [Fig. 2(d)]. In the latter case, there is no specific heat jump [25], and the $3DXY$ critical fluctuations induce the nonanalytical behavior of the specific heat across the λ transition [3]. Thus, what distinguishes the case of field-induced states of graphite from a typical superconductor and the archetypal superfluid is the simultaneous presence of a BCS jump and strong fluctuations and the contrasting evolution of these two components of the specific heat anomaly in a narrow field range.

Figure 4(a) shows ΔC_{el} as a function of the reduced temperature $\tau = T - T_c^p/T_c^p$. ΔC_{el} quantifies the excess in specific heat relative to a mean-field transition. The log-log plot shows that $\Delta C_{el}(\tau > 0)$ does not evolve as a power law

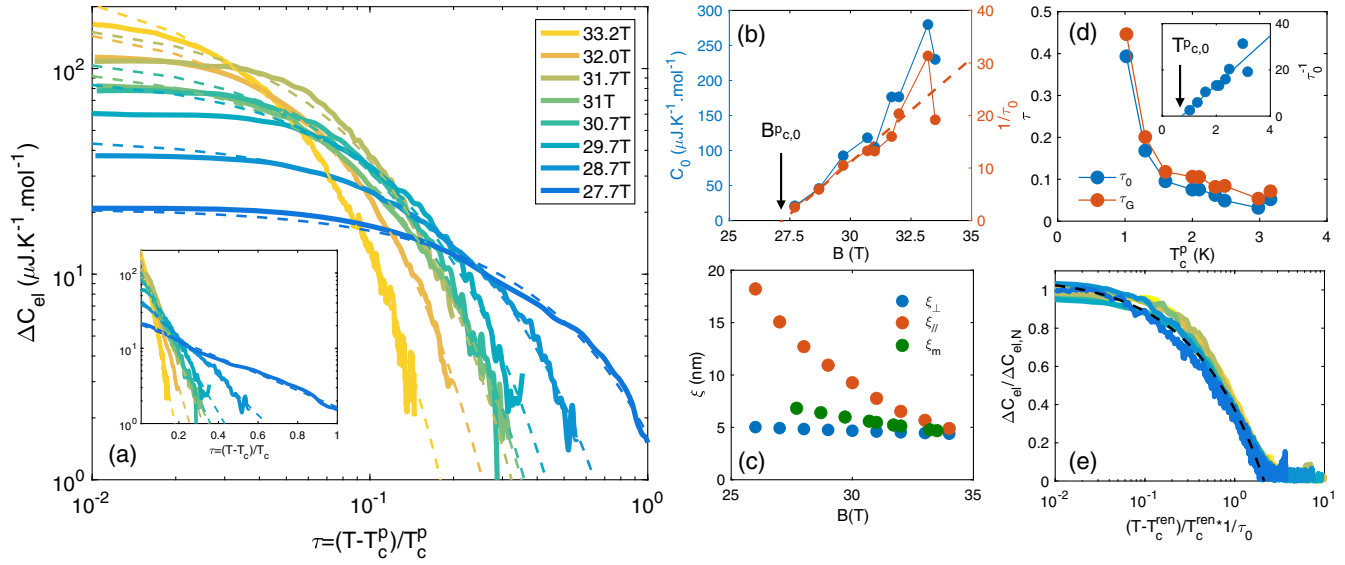

FIG. 4. Fluctuations regime of the electronic specific heat. (a) $\Delta C_{\rm el} = C_{\rm el} - \gamma_N T$ as a function of $\tau = T - T_c/T_c$ for $\tau > 0$. The dashed line correspond to a phenomenological fit $\Delta C_{\rm el} = C_0 \exp(-(\tau/\tau_0))$. Inset: $\ln(\Delta C_{\rm el})$ as a function of τ. (b) Field dependence of C_0 and τ_0^{-1}. The red dot line is linear fit of τ_0^{-1}. (c) Field dependence of $\xi_\perp = \ell_B$, $\xi_{//} = \xi_0$ (see text), and $\xi_m = (\xi_\perp^2 \xi_{//})^{1/3}$. (d) Temperature dependence of τ_0 compared to τ_G. Inset: plot τ_0^{-1} vs T_c^p with a linear fit (blue line). (e) Normalized plot $\Delta C_{\rm el}$ as function of $(T - T_c^{\rm ren})/T_c^{\rm ren}\tau_0$, where $T_c^{\rm ren}$ is a renormalized $T_c^{\rm ren} = T_c^p(1 + 0.5\tau_0)$. The black dot line is a fit with the $3DXY$ model (see text and [17]).

and points therefore to a non-Gaussian origin (for which $\Delta C_{\rm el}^{\rm Gauss.} = 1/\xi_0^D \tau^{2-D/2}$, where D is the dimension and ξ_0 is the BCS coherence length [26]). However, as shown in the inset of the same figure, an empirical law of the form $\Delta C_{\rm el} = C_0 \exp(-(\tau/\tau_0))$ captures the evolution of the data with B and τ. The field dependence of both parameters δC_0 and τ_0 is shown in Fig. 4(b). With a decreasing magnetic field, τ_0 increases, and its extrapolation implies $\tau_0^{-1} = 0$ when $B < 27$ T. In this case, no specific heat anomaly is detected down to 0.6 K [Fig. 2(a)]. It is possible to collapse all the curves on top of each other by plotting $\Delta C_{\rm el}/C_0$ vs $(T - T_c^{\rm ren})/T_c^{\rm ren}\tau_0$, where $T_c^{\rm ren}$ is a renormalized T_c^p equal to $T_c^p(1 + 0.5\tau_0)$ [Fig. 4(e)].

The success of this simple scaling procedure has implications for the origin of the broadening of the transition caused by a small variation in the amplitude of the magnetic field. It is unlikely that disorder plays a major role. In this layered material, however, the in-plane and out-of-plane length scales differ by several orders of magnitude. The mean free path within the graphene planes $\ell_e^\perp$ is very long, in the range of 5 to 50 μm, 3 orders of magnitude longer than $k_{F,\perp}^{-1} = 7$ nm and the magnetic length $\ell_B = \sqrt{(\hbar/eB)} = 5$ nm at 25 T, which is a plausible candidate to represent the in-plane coherence length ($\xi_\perp$) when $B > B_{\rm QL}$. The mean free path along the c axis, $\ell_e^{//}$, is 2 or 3 orders of magnitude shorter than $\ell_e^\perp$. However, this path remains longer than the c-axis interelectron distance $d_{e-e,//} \simeq k_{F,//}^{-1} \simeq 1$ nm and exceeds the c-axis coherence length ($\xi_{//}$), which can be estimated using the BCS coherence length $\xi_0 = \hbar^2 k_{F,//}/\pi m_z^\star \Delta_c$. Δ_c is the c-axis gap [deduced from the activated behavior of R_{zz} and shown in the inset of Fig. 3(b)] and $k_{F,//} = \pi/4a$ (where a is the interlayer distance). As seen in Fig. 4(d), $\xi_{//}(33{\rm T}) \simeq 5$ nm and $\xi_{//}(25{\rm T}) \simeq 15$ nm. The latter number may approach the estimated $\ell_e^{//}$ below 25 T. Therefore, the role played by stacking disorder across the planes in causing the broadening cannot be ruled out at the lowest magnetic field.

The most plausible source of the observed broadening is critical fluctuations. This can be quantified by the Ginzburg criterion. Plugging the measured $\Delta C_{\rm el}(T_c^p)$ and the estimated $\xi_{//,\perp}$ [$\xi_m = (\xi_{//}^2 \xi_\perp)^{1/3}$] in Eq. (1), we deduce τ_G. This estimation of τ_G closely matches the τ_0 deduced from our fits to the data [Fig. 4(d)]. At the highest field, $B = 33$ T $\tau_G \simeq 0.05$, which is nonnegligible. As the field decreases to 27.7 T, τ_G becomes as large as 0.45, which is exceptionally large in comparison to any other known second-order phase transition. Table I compares our case to a few other systems. The list consists of a conventional superconductor (Sn), two superconductors with a higher T_c and shorter coherence lengths (MgB_2 and YBa_2CuO_7), and a charge density wave (CDW) solid ($K_{0.3}MoO_3$). Graphite is a system in which 10 000 atoms share a single electron and hole, hence its small $\Delta C_{\rm el}(T_c^p)$. Even at 33 T, the amplitude of the specific heat jump is many orders of magnitude smaller than for the other systems. This $\Delta C_{\rm el}(T_c^p) \simeq 0.16$ mJK^{-1} mol^{-1} (combined with a molar volume of $V_m = 5.27$ cm$^3 \cdot$ mol^{-1}) implies that the difference in average specific heat of the normal and ordered

TABLE I. Comparison of $\tau_G = 1/32\pi^2(k_B/\Delta C\xi_0^3)^2$ for different superconductors (SC) (Sn, MgB_2, and YBa_2CuO_7), the CDW system ($K_{0.3}MoO_3$), and in graphite. $\Delta C = \Delta C_{el}(T_c) \times V_m$ is the amplitude of the jump of specific heat at the transition in $J.K^{-1}.m^{-3}$, V_m is the molar volume, and ξ_0 is the BCS coherence length. For anisotropic compounds, the average value of ξ_0, ξ_m, is used.

Sample	$\Delta C(J.K^{-1}.m^{-3})$	ξ_0(Å)	τ_G
Sn (SC) [1]	800	2300	10^{-14}
MgB_2 (SC) [27]	3360	26	10^{-3}
$K_{0.3}MoO_3$ (CDW) [28,29]	35800	$6.2(\xi_m)$	0.01
YBa_2CuO_7 (SC) [30]	4993	$6.7(\xi_m)$	0.2
Graphite (33.2 T)	30.1	$47(\xi_m)$	0.05
Graphite (27.7 T)	3.7	$68(\xi_m)$	0.45

phases within a coherence volume becomes comparable to k_B ($\Delta C\xi_m^3 \simeq 0.3k_B$), making this competition critically fragile. With a decreasing magnetic field, fluctuations grow and the transition widens because of further decrease in $\Delta C_{el}(T_c^p)$.

So far we have discussed the temperature dependence of ΔC_{el} through a phenomenological two-parameter exponential fit. On the whole temperature range, it is equally possible to fit ΔC_{el} with a simplified version of the asymptotic form of the $3DXY$ universality class expression with three parameters [Fig. 4(e)]: $A_0(1 + C_0|\tau^{0.5}| + D_0\tau)$ (see [17]). This universality class provides a natural explanation for the saturation of ΔC_{el} at low τ due to its almost vanishing critical exponent ($\alpha \approx -0.01$ [31]). Therefore, we conclude that the observed broadening of the transition is caused by critical fluctuations belonging to the $3DXY$ model. The Gaussian fluctuations expected outside the critical window, i.e., for $\tau > \tau_G$, would bring a correction to the mean-field behavior. Such a correction is not detected in our data, presumably because of the width and predominance of the critical fluctuations.

These results help in understanding the evolution of the observed anomalies in the Nernst effect [12,32] (a measure of the entropy per carrier [33]) and ultrasound measurements [13] caused by the transition. At low temperatures, one expects that ordering induces a smooth variation in entropy (see [17]) and therefore a rounded drop in the Nernst response [12,32]. As the temperature increases, the mean-field component of the transition strengthens, and the Nernst anomaly becomes a clear kink. Furthermore, the origin of the relatively large jump in the sound velocity becomes clear. It has been argued [13] that the relative large jump in the sound velocity can be caused by either a strong anisotropy in the strain dependence of T_c or a large jump in the specific heat (e.g., due to a putative lattice deformation accompanying the transition). According to this study, $\Delta C_{el}(T_c^p) \approx \gamma_N T_c$, and the transition is purely electronic. Therefore, we can safely conclude that the jump in the sound velocity is caused by a strong anisotropic strain dependence of T_c.

Future studies of the specific heat in higher magnetic fields would shed light on the BCS–Bose-Einstein condensation crossover as one approaches the maximum transition temperature around 47 T, where the degeneracy and critical temperatures become similar [32]. Specific heat studies on other dilute metals pushed to extreme quantum limits and hosting field-induced states (such as bismuth [34,35], InAs [36], TaAs [37], or $ZrTe_5$ [38]) could bring interesting insights.

In summary, we measured the specific heat of graphite in a high magnetic field and detected a second-order phase transition jump. The specific heat anomaly drastically evolves in a narrow field window due to the change in the balance between critical fluctuations and a mean-field jump. The field-induced phase transition in graphite emerges from this study as possessing an exceptionally wide critical window compared to any other electronic phase transition.

We thank I. Paul and Z. Zhu for useful discussions. We acknowledge the support of the LNCMI-CNRS, a member of the European Magnetic Field Laboratory (EMFL). This work was supported by Jeunes Equipes de l'Institut de Physique du Collège de France-Collège de France, by the Agence Nationale de la Recherche (ANR-18-CE92-0020-01; ANR-19-CE30-0014-04), and by a grant contributed by the Ile de France regional council. J. K. was supported by the Slovak Research and Development Agency (SRDA) Grants No. APVV-16-0372 and No. VEGA 2/0058/20.

*Corresponding author.
benoit.fauque@espci.fr

[1] L. P. Kadanoff, W. Götze, D. Hamblen, R. Hecht, E. A. S. Lewis, V. V. Palciauskas, M. Rayl, J. Swift, D. Aspnes, and J. Kane, Rev. Mod. Phys. **39**, 395 (1967).
[2] V. Ginzburg, Sov. Phys. Solid State **2**, 1824 (1960).
[3] J. A. Lipa, D. R. Swanson, J. A. Nissen, T. C. P. Chui, and U. E. Israelsson, Phys. Rev. Lett. **76**, 944 (1996).
[4] S. Sachdev, *Quantum Phase Transitions* (Cambridge University Press, Cambridge, England, 2011).
[5] S. Tanuma, R. Inada, A. Furukawa, O. Takahashi, Y. Iye, and Y. Onuki, *Springer Series in Solid State Sciences* (Springer, Berlin, 1981).
[6] H. Yaguchi and J. Singleton, Phys. Rev. Lett. **81**, 5193 (1998).
[7] B. Fauqué, D. LeBoeuf, B. Vignolle, M. Nardone, C. Proust, and K. Behnia, Phys. Rev. Lett. **110**, 266601 (2013).
[8] K. Akiba, A. Miyake, H. Yaguchi, A. Matsuo, K. Kindo, and M. Tokunaga, J. Phys. Soc. Jpn. **84**, 054709 (2015).
[9] Z. Zhu, R. D. McDonald, A. Shekhter, B. J. Ramshaw, K. A. Modic, F. F. Balakirev, and N. Harrison, Sci. Rep. **7**, 1733 (2017).
[10] F. Arnold, A. Isidori, E. Kampert, B. Yager, M. Eschrig, and J. Saunders, Phys. Rev. Lett. **119**, 136601 (2017).

[11] Z. Zhu, P. Nie, B. Fauqué, B. Vignolle, C. Proust, R. D. McDonald, N. Harrison, and K. Behnia, Phys. Rev. X **9**, 011058 (2019).
[12] B. Fauqué, Z. Zhu, T. Murphy, and K. Behnia, Phys. Rev. Lett. **106**, 246405 (2011).
[13] D. LeBoeuf, C. W. Rischau, G. Seyfarth, R. Küchler, M. Berben, S. Wiedmann, W. Tabis, M. Frachet, K. Behnia, and B. Fauqué, Nat. Commun. **8**, 1337 (2017).
[14] D. Yoshioka and H. Fukuyama, J. Phys. Soc. Jpn. **50**, 725 (1981).
[15] Y. Takada and H. Goto, J. Phys. Condens. Matter **10**, 11315 (1998).
[16] Z. Pan and R. Shindou, Phys. Rev. B **100**, 165124 (2019).
[17] See Supplemental Material, which includes Refs. [18–20], at http://link.aps.org/supplemental/10.1103/PhysRevLett.126.106801 for more details on the sample, a discussion of the density of state and the electronic specific heat of 3D metals in the quantum limit, the *c*-axis transport measurement, and the fit of ΔC_{el} with the $3DXY$ model.
[18] D. Tsang and M. Dresselhaus, Carbon **14**, 43 (1976).
[19] J. M. Ziman, *Principle of the Theory of Solids* (Cambridge University Press, Cambridge, England, 1972).
[20] M. Campostrini, M. Hasenbusch, A. Pelissetto, P. Rossi, and E. Vicari, Phys. Rev. B **63**, 214503 (2001).
[21] K. Komatsu and T. Nagamiya, J. Phys. Soc. Jpn. **6**, 438 (1951).
[22] B. J. C. van der Hoeven and P. H. Keesom, Phys. Rev. **130**, 1318 (1963).
[23] A. W. Rost, S. A. Grigera, J. A. N. Bruin, R. S. Perry, D. Tian, S. Raghu, S. A. Kivelson, and A. P. Mackenzie, Proc. Natl. Acad. Sci. U.S.A. **108**, 16549 (2011).
[24] J.-P. Jay-Gerin, Solid State Commun. **19**, 1241 (1976).
[25] R. P. Feynman, Phys. Rev. **91**, 1291 (1953).
[26] A. Larkin and A. Varlamov, *Theory of Fluctuations in Superconductors* (Oxford University Press, New York, 2005).
[27] T. Park, M. B. Salamon, C. U. Jung, M.-S. Park, K. Kim, and S.-I. Lee, Phys. Rev. B **66**, 134515 (2002).
[28] J. W. Brill, M. Chung, Y. K. Kuo, X. Zhan, E. Figueroa, and G. Mozurkewich, Phys. Rev. Lett. **74**, 1182 (1995).
[29] R. H. McKenzie, Phys. Rev. B **51**, 6249 (1995).
[30] A. Junod, Y. Wang, F. Bouquet, and P. Toulemonde, in *Studies of High Temperature Superconductors, Nova Science Publishers,*, edited by A. Narlikar (Nova Science Publishers, Commack, NY, 2002), p. 179.
[31] J. C. Le Guillou and J. Zinn-Justin, J. Phys. Lett. **46**, 137 (1985).
[32] J. Wang, P. Nie, X. Li, H. Zuo, B. Fauqué, Z. Zhu, and K. Behnia, Proc. Natl. Acad. Sci. U.S.A. **117**, 30215 (2020).
[33] D. L. Bergman and V. Oganesyan, Phys. Rev. Lett. **104**, 066601 (2010).
[34] Z. Zhu, J. Wang, H. Zuo, B. Fauqué, R. D. McDonald, Y. Fuseya, and K. Behnia, Nat. Commun. **8**, 15297 (2017).
[35] A. Iwasa, A. Kondo, S. Kawachi, K. Akiba, Y. Nakanishi, M. Yoshizawa, M. Tokunaga, and K. Kindo, Sci. Rep. **9**, 1672 (2019).
[36] A. Jaoui, G. Seyfarth, C. W. Rischau, S. Wiedmann, S. Benhabib, C. Proust, K. Behnia, and B. Fauqué, npj Quantum Mater. **5**, 94 (2020).
[37] B. J. Ramshaw, K. A. Modic, A. Shekhter, Y. Zhang, E.-A. Kim, P. J. W. Moll, M. D. Bachmann, M. K. Chan, J. B. Betts, F. Balakirev, A. Migliori, N. J. Ghimire, E. D. Bauer, F. Ronning, and R. D. McDonald, Nat. Commun. **9**, 2217 (2018).
[38] F. Tang, Y. Ren, P. Wang, R. Zhong, J. Schneeloch, S. A. Yang, K. Yang, P. A. Lee, G. Gu, Z. Qiao, and L. Zhang, Nature (London) **569**, 537 (2019).